Journal of Photonics for Energy

PhotonicsforEnergy.SPIEDigitalLibrary.org

Design concepts for hot carrier-based detectors and energy converters in the near ultraviolet and infrared

Tao Gong
Lisa Krayer
Jeremy N. Munday

SPIE.

Tao Gong, Lisa Krayer, Jeremy N. Munday, "Design concepts for hot carrier-based detectors and energy converters in the near ultraviolet and infrared," *J. Photon. Energy* **6**(4), 042510 (2016), doi: 10.1117/1.JPE.6.042510.

Design concepts for hot carrier-based detectors and energy converters in the near ultraviolet and infrared

Tao Gong,[a,b] Lisa Krayer,[a,b] and Jeremy N. Munday[a,b,*]

[a]University of Maryland, Department of Electrical and Computer Engineering, College Park, Maryland 20742-3511, United States

[b]University of Maryland, Institute for Research in Electronics and Applied Physics, College Park, Maryland 20742-3511, United States

Abstract. Semiconductor materials are well suited for power conversion when the incident photon energy is slightly larger than the bandgap energy of the semiconductor. However, for photons with energy significantly greater than the bandgap energy, power conversion efficiencies are low. Further, for photons with energy below the bandgap energy, the absence of absorption results in no power generation. Here, we describe photon detection and power conversion of both high- and low-energy photons using hot carrier effects. For the absorption of high-energy photons, excited electrons and holes have excess kinetic energy that is typically lost through thermalization processes between the carriers and the lattice. However, collection of hot carriers before thermalization allows for reduced power loss. Devices utilizing plasmonic nanostructures or simple three-layer stacks (transparent conductor–insulator–metal) can be used to generate and collect these hot carriers. Alternatively, hot carrier collection from sub-bandgap photons can be possible by forming a Schottky junction with an absorbing metal so that hot carriers generated in the metal can be injected across the semiconductor–metal interface. Such structures enable near-IR detection based on sub-bandgap photon absorption. Further, utilization and optimization of localized surface plasmon resonances can increase optical absorption and hot carrier generation (through plasmon decay). Combining these concepts, hot carrier generation and collection can be exploited over a large range of incident wavelengths spanning the UV, visible, and IR. © *2016 Society of Photo-Optical Instrumentation Engineers (SPIE)* [DOI: 10.1117/1.JPE.6.042510]

Keywords: hot carriers; plasmonics; photonics; photovoltaics; solar cells; detectors.

Paper 16080SSP received Jul. 1, 2016; accepted for publication Aug. 25, 2016; published online Sep. 21, 2016.

1 Introduction

The field of plasmonics, which involves the coupling of light and free electron charge densities, has evolved rapidly over the past decade as a result of advances in nanofabrication techniques. Metallic nanostructures have enabled high-electromagnetic field intensities near metal interfaces and have led to a range of devices including modulators, lasers, amplifiers, detectors, sensors, nanocircuit elements, and so on.[1–15] Surface plasmon interactions can typically be divided into two categories: localized surface plasmons and propagating surface plasmon polaritons. For both cases, an incident electromagnetic wave couples to the free charges in the metal and creates a coupled oscillation at the metal–dielectric interface. These oscillations are typically confined to a small volume and lead to high field intensities. Larger metallic particles (~100 nm) cause enhanced scattering of the incident light while smaller particles (~10 nm) lead to enhanced absorption.[16,17]

Traditionally, plasmonic structures have been applied to photovoltaic (PV) devices to increase the absorption within the semiconductor. However, the emerging field of hot carrier plasmonics is fundamentally different because the light is absorbed within the metal to generate

*Address all correspondence to: Jeremy N. Munday, E-mail: jnmunday@umd.edu

1947-7988/2016/$25.00 © 2016 SPIE

carriers; therefore, the devices are based on metallic absorption rather than semiconductor absorption. Figure 1 shows the two basic structures that have been used to generate and collect hot carriers in metals: (1) metal–insulator–metal (M–I–M) structures and (2) metal–semiconductor (M–S) Schottky junctions. In either case, light is incident on the structure and is predominantly absorbed in one metallic contact [the left contact in Fig. 1(a)], which is nanostructured to excite surface plasmons. The absorption either leads to the direct generation of carriers with excess kinetic energy, i.e., the so-called hot carriers, or to surface plasmons, which subsequently decay into hot carriers. These carriers will diffuse, and a fraction of them will find their way to the dielectric or semiconductor interface and will traverse it. For the M–I–M structure, a net current will flow based on the absorption profile within each metal and on the voltage established by the energy barrier for carriers to travel from one metal to the other. A similar effect is found for M–S devices with a Schottky junction.

Hot carrier devices have several advantages over ones based on semiconductors alone. Specific benefits include tunable absorption, higher energy transfer per incident photon due to selective collection of high-energy carriers, generation of carriers from sub-bandgap photons, and short thermalization times,[18–21] which have been used to alter chemical processes,[22–24] to enable advanced energy conversion and photon detection,[25–35] for nanoscopy,[36] to modify thermally induced processes,[37–39] to induce structure phase transition,[40] and so on.

2 Semiconductor-Free Hot Carrier Devices

Traditional photodetectors rely on semiconductor absorption to generate electron-hole pairs that result in photocurrent; however, hot carrier devices that exploit metallic absorption do not need to include a semiconductor. Thus, simple structures can be constructed out of metals and dielectrics to achieve hot carrier current upon photoexcitation.

To determine the expected photocurrent from semiconductor-free hot carrier plasmonic devices, we simulated the response of various M–I–M structures using the theory described in Refs. 25 and 29. Figure 2 shows two devices: an M–I–M device based on a transparent conducting electrode (indium tin oxide, ITO) and a grating-based M–I–M device. Both structures result in preferential photon absorption on one side of the device. The M–I–M based on a transparent conducting electrode benefits from ease of fabrication while maintaining large absorption of short wavelengths, whereas the grating structure provides an absorption spectrum with tunable resonances determined by the pitch, width, and height of the grating [Fig. 2(d)]. For a planar ITO − Al_2O_3 − Au structure [Fig. 2(a)], nearly all the absorptions occur in the Au layer, making it an excellent candidate for a hot carrier plasmonic device. Light incident on the device passes

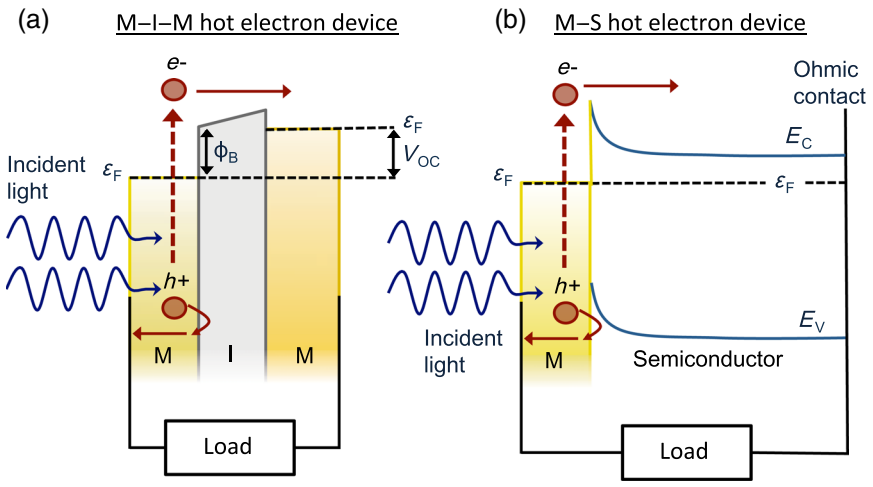

Fig. 1 Schematic diagrams showing the operational principle of hot carrier plasmonic devices. (a) Absorption in the first layer of a metal–insulator–metal (M–I–M) device generates hot electrons with kinetic energy great enough to traverse the insulating gap. (b) Illustration of a metal–semiconductor (M–S) hot carrier plasmonic device based on a Schottky interface.

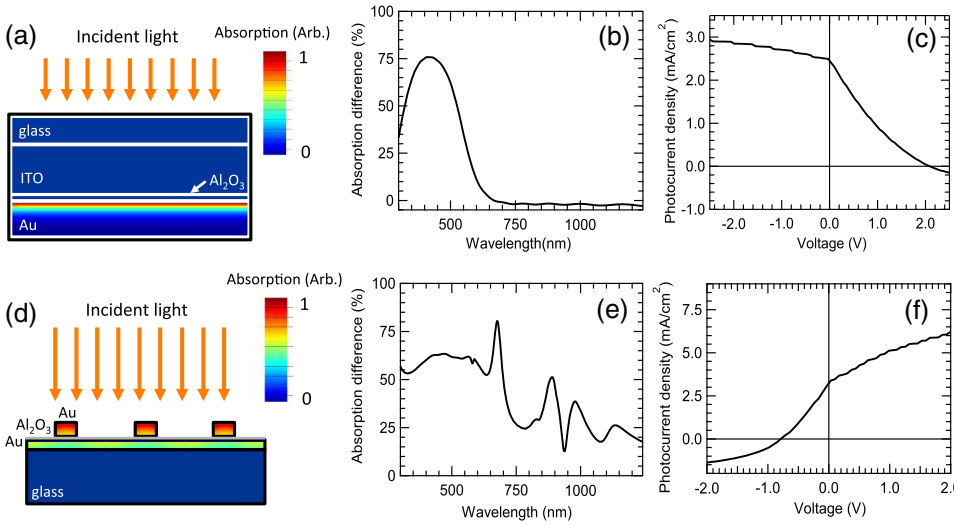

Fig. 2 Optoelectronic simulations of hot carrier plasmonic devices. (a) Absorption simulation for an ITO – Al_2O_3 – Au planar structure. High absorption is shown only on the Au side of the Au – Al_2O_3 interface. (b) The absorption difference between gold and ITO is large at short wavelengths. (c) Photocurrent–voltage characteristic shows photodetector's expected response and power generation (upper right quadrant of the current–voltage characteristic for this device). The applied voltage is the relative voltage drop between the bottom electrode and top electrode (grounded). (d) Absorption profile for a grating device coated with a thin layer of ITO on top as the top electrode. The width and height of the grating are 500 and 50 nm, respectively, and the period is 600 nm. (e) Preferential absorption occurs in the grating, leading to a large absorption difference and hence the hot carriers flow from the grating to the thin film. (f) Photocurrent–voltage characteristic for the structure showing power generation in the upper left quadrant. Note the photocurrent increases as the applied voltage increases, which is different from (c). This is because the top layer is the main absorber in this case.

through the glass, ITO, and Al_2O_3 with negligible absorption (<1%). Upon striking the Au surface, an appreciable amount of light is absorbed within the first 20 to 40 nm of the film (e.g., ~70% of the 460-nm light is absorbed within the first 30 nm). This satisfies two important criteria for an M–I–M hot carrier device: preferential absorption in only one conductor and absorption near the conductor–insulator interface. The simulated transparent conducting electrode device has a power conversion efficiency of ~3% for 400-nm illumination and can reach ~11% if the electron density of states is modified.[25,32,41–43] Further details about this device can be found in Ref. 25.

In order to achieve a large net photoresponse from an M–I–M hot carrier device, an asymmetric absorption profile is necessary. Further, the absorption should occur near the metal–insulator interface to aid in carrier traversal across the insulating barrier. In Fig. 2, the asymmetric absorption profile was obtained through either the use of a transparent metal contact (ITO), which absorbs negligible amounts of the incident light, or through the coupling to grating resonances, which yields higher fields and absorption in the grating compared with the thin Au film.

Many M–I–M geometries are possible, and we highlight three examples (Fig. 3). A planar geometry is the simplest to fabricate; however, achieving strong absorption in only one layer near the metal–insulator interface is difficult. Two routes have shown promise: (1) through the use of a low absorption, transparent conducting layer as discussed above[25] or (2) through prism coupling to propagating surface plasmon modes.[29] A second promising direction is the use of nanoparticles or gratings.[27] Depending upon the design, the nanostructures can be used to either absorb the incident light or to scatter the light into the lower layer, where it is absorbed [Fig. 3(b)]. A third option is the use of vertical nanostructures such as nanowires or nanotubes. Nanowire arrays have proven advantages for PV applications because they enable a decoupling of the absorption length and the carrier diffusion length, because light is absorbed in the vertical direction while carriers are collected horizontally. Similar advantages can be achieved for hot carrier devices [Fig. 3(c)].

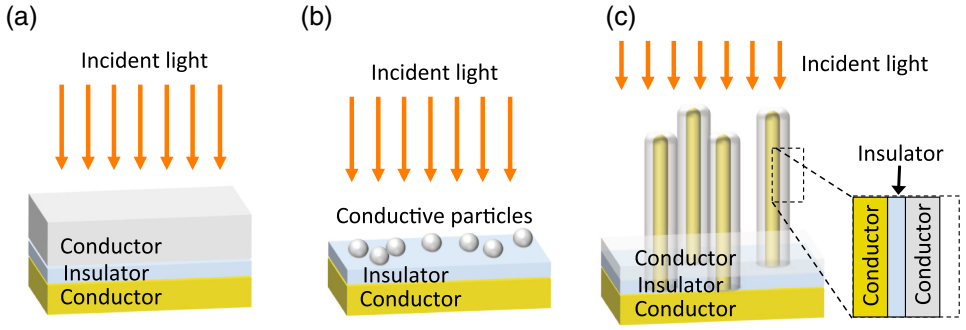

Fig. 3 Three simple geometries for light absorption and subsequent hot carrier collection: (a) planar, (b) nanoparticle, and (c) three-dimensional nanowire or vertical nanostructure.

3 Sub-bandgap Photocurrent in Semiconductors

In addition to M–I–M structures, M–S devices composed of metal nanostructures on a semiconductor can also lead to hot carrier excitation in the metal and subsequent collection within the semiconductor.[31,44] Because the absorption is in the metal rather than the semiconductor, the incident photons do not need to have energy greater than the semiconductor bandgap energy in order to generate carriers. Thus, hot electron injection can enable sub-bandgap photodetection.

Figure 4 shows one such device: a near-IR detector made from Si and Au, with illumination from the Si side. As the period is increased, the absorption (which occurs in the metal) is red-shifted. As a result, the absorption peak can be tuned throughout the near IR where the Si is nonabsorbing. The energetic carriers excited within the Au are injected into the Si and collected by an ohmic contact. For photons with sufficiently low energy ($\lambda > 2\ \mu$m), carrier injection can be aided by the application of an applied external bias.

4 Hot Carrier Energy Converters

A large discrepancy exists between the maximum solar energy conversion efficiency predicted by the Carnot limit (95%) and that of the best-reported nonconcentrating single-junction solar cell (28.8%).[45] This difference arises as a result of both extrinsic losses (e.g., series resistance, parasitic recombination, contact shadowing, and so on) and intrinsic losses (e.g., fundamental thermodynamic losses).[46] Extrinsic loss accounts for less than 3% of the total loss in the record GaAs single-junction solar cell; however, the intrinsic thermalization and sub-bandgap photon loss account for ~46% loss in efficiency.

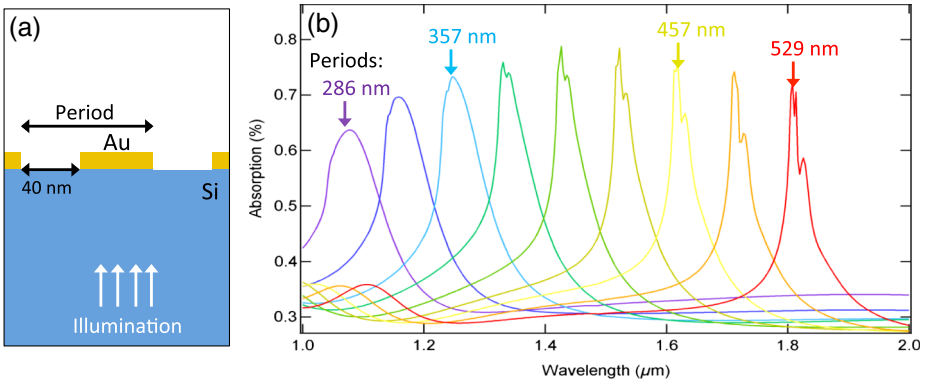

Fig. 4 Tunable hot carrier plasmon photodetector. (a) Schematic of a Si–Au-based device capable of detecting sub-bandgap photons due to plasmonic excitation and hot carrier injection into the Si. (b) Simulated absorption for the structure in (a) with an Au height of 15 nm and varied periodicity. As the period is increased, the absorption peak is red-shifted toward the IR.

The thermalization loss is the result of the energy mismatch between the energy of the incident photon and the energy of the collected electron-hole pair (see Fig. 5). A typical solar cell is made from a semiconductor with a $p-n$ junction (in addition to window layers), which is able to absorb photons above the semiconductor bandgap energy. The absorption results in the generation of carriers, which can be collected. If the incident photon has energy in excess of the bandgap energy, that energy is transferred to the excited carriers; however, the carriers will quickly (on the timescale of pico- to nanoseconds) relax down to the semiconductor bandgap through the emission of phonons, i.e., lattice vibrations. These phonons generally represent a large loss mechanism. For example, if a 3.0-eV photon is incident on a 1.1-eV bandgap semiconductor, an energy loss of 1.9 eV is expected. Additionally, if the incident photon has energy below the energy of the semiconductor bandgap, all the photon's energy will be lost due to its inability to excite electron-hole pairs in the semiconductor.

In order to avoid these losses, a number of approaches have been attempted. The most successful approach to date is the use of multiple semiconductors with different bandgaps.[47–57] This approach allows one to reduce the energy mismatch between the semiconductor bandgap and the incident photon energy by sending photons within a specific energy band to a particular bandgap material. Each material contains a $p-n$ junction, which can be connected electrically to form a multijunction device. This approach has resulted in a record solar cell with an efficiency of 46%,[58] recovering an additional 17.2% of the total possible power when compared with the record single-junction device. In order to achieve efficiencies greater than 50%, further material developments are needed.[50,52,59]

There are other approaches to recovering the energy loss due to thermalization, such as multicarrier excitation[60–67] and semiconductor-based hot carrier collection.[68–76] Carrier multiplication effects are similar to impact ionization effects in traditional semiconductors;[77] however, these effects are typically very small in bulk materials. In nanoscale semiconductor structures (e.g., quantum dots), quantum confinement effects can amplify this phenomenon to a measureable amount. Collection of hot electrons from a semiconductor has proven difficult due to short thermalization times (approximately picoseconds); however, results of Kempa et al.[73] suggest that these effects are observable in ultrathin semiconductor film devices. As described in this manuscript, hot carrier generation/collection in metals is a promising alternative to these concepts.

While efficiencies of >80% are the ultimate goal, plasmonic devices can be used in conjunction with traditional PV devices to improve their efficiencies. Figure 6 shows a hybrid hot carrier plasmonic device coupled to a traditional solar cell. Rather than capturing all the light in the plasmonic structure, the metal in the M–I–M device is only used to capture high-energy photons that are typically lost in a standard PV device (e.g., due to absorption in the passivating window layer), and separately, the sub-bandgap photons are captured in the M–S device. Figure 6 shows one example, but various tandem or spectrum splitting schemes

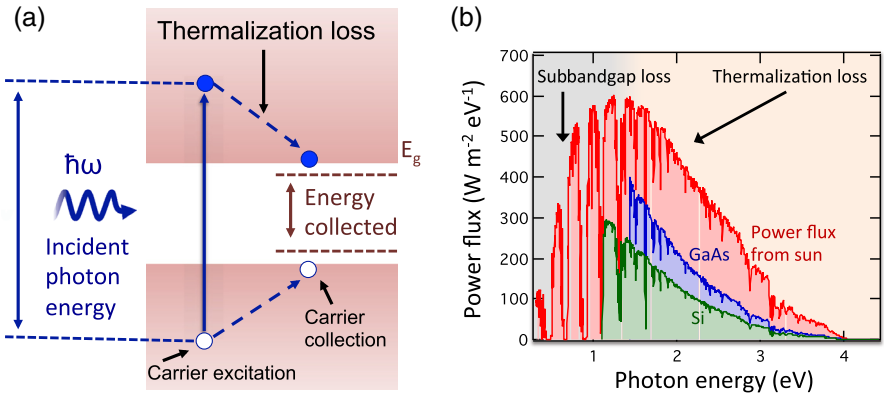

Fig. 5 Thermalization loss mechanism. (a) Absorption of a high-energy photon results in energy loss as the carrier relaxes down to the semiconductor bandgap. (b) Incident power flux from the sun (red) compared with the generated power flux from GaAs (blue) and Si (green). Power is lost from high-energy photons due to thermalization. Low-energy photons result in a loss due to their inability to excite electron-hole pairs.

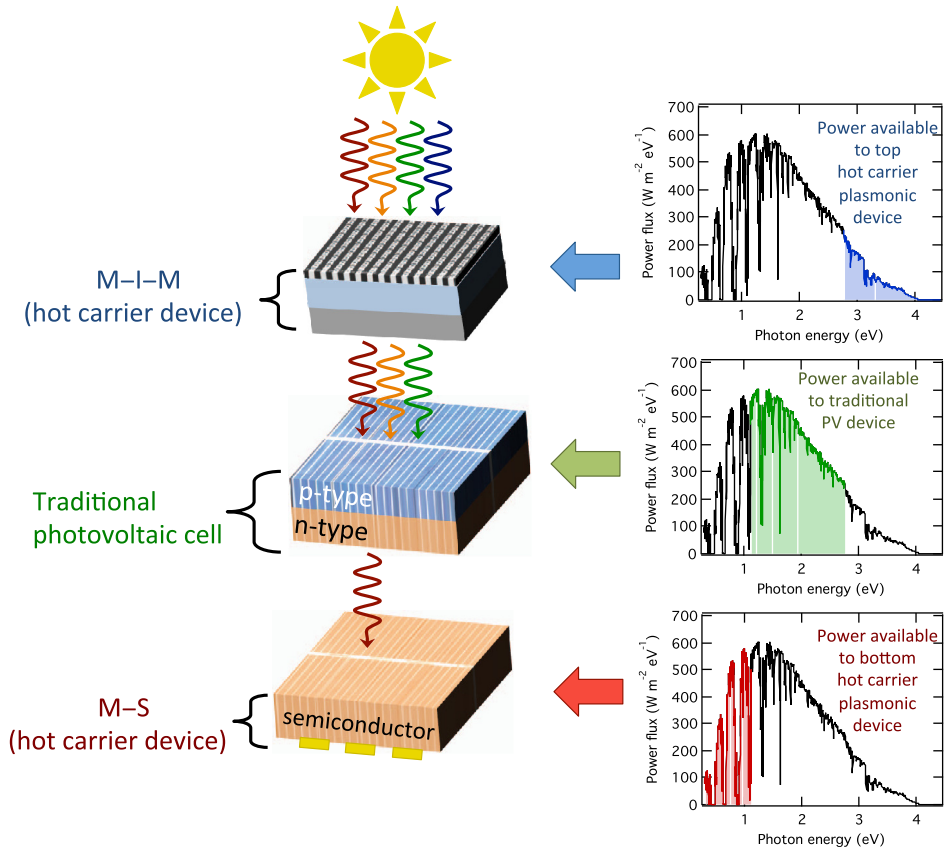

Fig. 6 Schematic of a hybrid hot carrier effect solar device. A traditional solar cell is used to absorb a fraction of the solar spectrum, and the hot carrier devices are used to capture photons that are usually inefficiently converted to energy in a traditional PV device. Thus, any added power generated by the plasmonic device will increase the total efficiency above that of the traditional PV device.

can be used. Here, the spectrum is broken up into three spectral regions and the photons are sent to the appropriate device.

5 Conclusions

Many opportunities exist for using hot carrier effects in metals to create new detectors and solar energy harvesters. By taking advantage of concepts developed in plasmonics, devices can be tuned throughout the UV, visible, and IR ranges using a combination of metals, semiconductors, and insulators. Due to the short thermalization timescales associated with carrier cooling, ultrafast detectors and sensors can be enabled using these concepts.

Acknowledgments

This work was funded in part by an Office of Naval Research YIP award under Grant No. 12044988 and the National Science Foundation under Grant No. ECCS-1554503.

References

1. P. Berini and I. De Leon, "Surface plasmon-polariton amplifiers and lasers," *Nat. Photonics* **6**, 16–24 (2012).
2. R.-M. Ma et al., "Plasmon lasers: coherent light source at molecular scales," *Laser Photonics Rev.* **7**, 1–21 (2013).
3. O. Hess et al., "Active nanoplasmonic metamaterials," *Nat. Mater.* **11**, 573–584 (2012).
4. J. N. Anker et al., "Biosensing with plasmonic nanosensors," *Nat. Mater.* **7**, 442–453 (2008).

5. V. Giannini et al., "Plasmonic nanoantennas: fundamentals and their use in controlling the radiative properties of nanoemitters," *Chem. Rev.* **111**, 3888–3912 (2011).
6. J. Lin et al., "Polarization-controlled tunable directional coupling of surface plasmon polaritons," *Science* **340**, 331–334 (2013).
7. N. Yu, Q. Wang, and F. Capasso, "Beam engineering of quantum cascade lasers," *Laser Photonics Rev.* **6**, 24–46 (2012).
8. P. Fan et al., "An electrically-driven GaAs nanowire surface plasmon source," *Nano Lett.* **12**, 4943–4947 (2012).
9. K. Diest et al., "Tunable color filters based on metal-insulator-metal resonators," *Nano Lett.* **9**, 2579–2583 (2009).
10. J. A. Dionne et al., "PlasMOStor: a metal-oxide-Si field effect plasmonic modulator," *Nano Lett.* **9**, 897–902 (2009).
11. S. P. Burgos, S. Yokogawa, and H. A. Atwater, "Color imaging via nearest neighbor hole coupling in plasmonic color filters integrated onto a complementary metal-oxide semiconductor image sensor," *ACS Nano* **7**, 10038–10047 (2013).
12. N. Engheta, A. Salandrino, and A. Alu, "Circuit elements at optical frequencies: nanoinductors, nanocapacitors, and nanoresistors," *Phys. Rev. Lett.* **95**, 095504 (2005).
13. A. Alu and N. Engheta, "Tuning the scattering response of optical nanoantennas with nanocircuit loads," *Nat. Photonics* **2**, 307–310 (2008).
14. M. W. Knight et al., "Aluminum plasmonic nanoantennas," *Nano Lett.* **12**, 6000–6004 (2012).
15. L. Zhou et al., "Aluminum nanocrystals as a plasmonic photocatalyst for hydrogen dissociation," *Nano Lett.* **16**, 1478–1484 (2016).
16. C. F. Bohren and D. R. Huffman, *Absorption and Scattering of Light by Small Particles*, John Wiley & Sons, New York (1983).
17. G. V. Hartland, "Optical studies of dynamics in noble metal nanostructures," *Chem. Rev.* **111**, 3858–3887 (2011).
18. A. Manjavacas et al., "Plasmon-induced hot carriers in metallic nanoparticles," *ACS Nano* **8**, 7630–7638 (2014).
19. A. M. Brown et al., "Nonradiative plasmon decay and hot carrier dynamics: effects of phonons, surfaces, and geometry," *ACS Nano* **10**, 957–966 (2016).
20. P. Narang, R. Sundararaman, and H. A. Atwater, "Plasmonic hot carrier dynamics in solid-state and chemical systems for energy conversion," *Nanophotonics* **5**, 96–111 (2016).
21. O. Demichel et al., "Dynamics, efficiency, and energy distribution of nonlinear plasmon-assisted generation of hot carriers," *ACS Photonics* **3**, 791–795 (2016).
22. S. Mubeen et al., "An autonomous photosynthetic device in which all charge carriers derive from surface plasmons," *Nat. Nanotechnol.* **8**, 247–251 (2013).
23. P. Christopher et al., "Singular characteristics and unique chemical bond activation mechanisms of photocatalytic reactions on plasmonic nanostructures," *Nat. Mater.* **11**, 1044–1050 (2012).
24. S. Mukherjee et al., "Hot electrons do the impossible: plasmon-induced dissociation of H_2 on Au," *Nano Lett.* **13**, 240–247 (2013).
25. T. Gong and J. N. Munday, "Angle-independent hot carrier generation and collection using transparent conducting oxides," *Nano Lett.* **15**, 147–152 (2015).
26. A. J. Leenheer et al., "Solar energy conversion via hot electron internal photoemission in metallic nanostructures: efficiency estimates," *J. Appl. Phys.* **115**, 134301 (2014).
27. H. Chalabi, D. Schoen, and M. L. Brongersma, "Hot-electron photodetection with a plasmonic nanostripe antenna," *Nano Lett.* **14**, 1374–1380 (2014).
28. J. Lee et al., "Plasmonic photoanodes for solar water splitting with visible light," *Nano Lett.* **12**, 5014–5019 (2012).
29. F. Wang and N. A. Melosh, "Plasmonic energy collection through hot carrier extraction," *Nano Lett.* **11**, 5426–5430 (2011).
30. N. Noginova et al., "Light-to-current and current-to-light coupling in plasmonic systems," *Phys. Rev. B* **84**, 035447 (2011).
31. M. W. Knight et al., "Photodetection with active optical antennas," *Science* **332**, 702–704 (2011).

32. T. P. White and K. R. Catchpole, "Plasmon-enhanced internal photoemission for photovoltaics: theoretical efficiency limits," *Appl. Phys. Lett.* **101**, 073905 (2012).
33. C. Clavero, "Plasmon-induced hot-electron generation at nanoparticle/metal-oxide interfaces for photovoltaic and photocatalytic devices," *Nat. Photonics* **8**, 95–103 (2014).
34. M. L. Brongersma, N. J. Halas, and P. Nordlander, "Plasmon-induced hot carrier science and technology," *Nat. Nanotechnol.* **10**, 25–34 (2015).
35. W. Wang et al., "Hot electron-based near-infrared photodetection using bilayer MoS_2," *Nano Lett.* **15**, 7440–7444 (2015).
36. A. Giugni et al., "Hot-electron nanoscopy using adiabatic compression of surface plasmons," *Nat. Nanotechnol.* **8**, 845–852 (2013).
37. J. M. Stern et al., "Selective prostate cancer thermal ablation with laser activated gold nanoshells," *J. Urol.* **179**, 748–753 (2008).
38. O. Neumann et al., "Solar vapor generation enabled by nanoparticles," *ACS Nano* **7**, 42–49 (2013).
39. K. J. Tielrooij et al., "Hot-carrier photocurrent effects at graphene-metal interfaces," *J. Phys.: Condens. Matter* **27**, 164207 (2015).
40. Y. Kang et al., "Plasmonic hot electron induced structural phase transition in a MoS_2 monolayer," *Adv. Mater.* **26**, 6467–6471 (2014).
41. E. Y. Chan, H. C. Card, and M. C. Teich, "Internal photoemission mechanisms at interfaces between germanium and thin metal films," *IEEE J. Quantum Electron.* **16**, 373–381 (1980).
42. R. Sundararaman et al., "Theoretical predictions for hot-carrier generation from surface plasmon decay," *Nat. Commun.* **5**, 5788 (2014).
43. T. Gong and J. N. Munday, "Materials for hot carrier plasmonics," *Opt. Mater. Express* **5**, 2501–2512 (2015).
44. F. P. G. de Arquer, A. Mihi, and G. Konstantatos, "Large-area plasmonic-crystal-hot-electron-based photodetectors," *ACS Photonics* **2**, 950–957 (2015).
45. M. A. Green et al., "Solar cell efficiency tables (version 43)," *Prog. Photovoltaics* **22**, 1–9 (2014).
46. L. C. Hirst and N. J. Ekins-Daukes, "Fundamental losses in solar cells," *Prog. Photovoltaics* **19**, 286–293 (2011).
47. S. Kurtz and J. Geisz, "Multijunction solar cells for conversion of concentrated sunlight to electricity," *Opt. Express* **18**, A73–A78 (2010).
48. T. G. J. Olson and M. Al-Jassim, "$GaInP_2$/GaAs-a current- and lattice-matched tandem cell with an high theoretical efficiency," in *Proc. 18th IEEE Photovoltaic Specialists Conf.*, pp. 552–555, New York (1985).
49. H. Cotal et al., "III-V multijunction solar cells for concentrating photovoltaics," *Energy Environ. Sci.* **2**, 174–192 (2009).
50. A. Luque and S. Hegedus, *Handbook of Photovoltaic Science and Engineering*, 2nd ed., John Wiley & Sons, Hoboken, New Jersey (2011).
51. K. A. Bertness et al., "29.5%-efficient GaInP/GaAs tandem solar cells," *Appl. Phys. Lett.* **65**, 989–991 (1994).
52. A. Luque, "Will we exceed 50% efficiency in photovoltaics?" *J. Appl. Phys.* **110**, 031301 (2011).
53. J. M. Olson et al., "A 27.3% efficient $Ga_{0.5}In_{0.5}P$/GaAs tandem solar cell," *Appl. Phys. Lett.* **56**, 623–625 (1990).
54. R. R. King et al., "40% efficient metamorphic GaInP/GaInAs/Ge multijunction solar cells," *Appl. Phys. Lett.* **90**, 183516 (2007).
55. J. F. Geisz et al., "High-efficiency GaInP/GaAs/InGaAs triple-junction solar cells grown inverted with a metamorphic bottom junction," *Appl. Phys. Lett.* **91**, 023502 (2007).
56. R. R. King et al., "Solar cell generations over 40% efficiency," *Prog. Photovoltaics* **20**, 801–815 (2012).
57. C. H. Henry, "Limiting efficiencies of ideal single and multiple energy gap terrestrial solar cells," *J. Appl. Phys.* **51**, 4494–4500 (1980).
58. "Record efficiency reported," http://www.nrel.gov/ncpv/images/efficiency_chart.jpg (14 June 2016).

59. M. S. Leite et al., "Towards an optimized all lattice-matched InAlAs/InGaAsP/InGaAs multijunction solar cell with efficiency >50%," *Appl. Phys. Lett.* **102**, 033901 (2013).
60. M. C. Hanna and A. J. Nozik, "Solar conversion efficiency of photovoltaic and photoelectrolysis cells with carrier multiplication absorbers," *J. Appl. Phys.* **100**, 074510 (2006).
61. J. A. McGuire et al., "Apparent versus true carrier multiplication yields in semiconductor nanocrystals," *Nano Lett.* **10**, 2049–2057 (2010).
62. C. Delerue et al., "Carrier multiplication in bulk and nanocrystalline semiconductors: mechanism, efficiency, and interest for solar cells," *Phys. Rev. B* **81**, 125306 (2010).
63. M. C. Beard et al., "Comparing multiple exciton generation in quantum dots to impact ionization in bulk semiconductors: implications for enhancement of solar energy conversion," *Nano Lett.* **10**, 3019–3027 (2010).
64. J. A. McGuire et al., "New aspects of carrier multiplication in semiconductor nanocrystals," *Acc. Chem. Res.* **41**, 1810–1819 (2008).
65. J. B. Sambur, T. Novet, and B. A. Parkinson, "Multiple exciton collection in a sensitized photovoltaic system," *Science* **330**, 63–66 (2010).
66. V. Sukhovatkin et al., "Colloidal quantum-dot photodetectors exploiting multiexciton generation," *Science* **324**, 1542–1544 (2009).
67. O. E. Semonin et al., "Peak external photocurrent quantum efficiency exceeding 100% via MEG in a quantum dot solar cell," *Science* **334**, 1530–1533 (2011).
68. R. T. Ross and A. J. Nozik, "Efficiency of hot-carrier solar energy converters," *J. Appl. Phys.* **53**, 3813–3818 (1982).
69. P. Wurfel, "Solar energy conversion with hot electrons from impact ionisation," *Sol. Energy Mater. Sol. Cells* **46**, 43–52 (1997).
70. P. Aliberti et al., "Investigation of theoretical efficiency limit of hot carriers solar cells with a bulk indium nitride absorber," *J. Appl. Phys.* **108**, 094507 (2010).
71. G. J. Conibeer et al., "Selective energy contacts for hot carrier solar cells," *Thin Solid Films* **516**, 6968–6973 (2008).
72. D. J. Farrell et al., "A hot-carrier solar cell with optical energy selective contacts," *Appl. Phys. Lett.* **99**, 111102 (2011).
73. K. Kempa et al., "Hot electron effect in nanoscopically thin photovoltaic junctions," *Appl. Phys. Lett.* **95**, 233121 (2009).
74. Y. Takeda et al., "Hot carrier solar cells operating under practical conditions," *J. Appl. Phys.* **105**, 074905 (2009).
75. W. A. Tisdale et al., "Hot-electron transfer from semiconductor nanocrystals," *Science* **328**, 1543–1547 (2010).
76. D. J. Farrell et al., "Can a hot-carrier solar cell also be an efficient up-converter?" *IEEE J. Photovoltaics* **5**, 571–576 (2015).
77. L. R. Canfield et al., "Absolute silicon photodiodes for 160 nm to 254 nm photons," *Metrologia* **35**, 329–334 (1998).

Tao Gong received his BS degree in physics from the University of Science and Technology of China in 2011. Currently, he is a PhD student in electrical and computer engineering at the University of Maryland, College Park. His interests include nanophotonics, plasmonics, hot carrier effects, and solar energy harvesting. He is a student member of SPIE and APS.

Lisa Krayer received her BS degree in physics from the University of California, San Diego, in 2013. She is a PhD student and NSF graduate research fellow in the Department of Electrical and Computer Engineering at University of Maryland, College Park. Her research interests include fabrication and characterization of hot carrier and plasmonic devices for solar energy harvesting. She is a student member of APS.

Jeremy N. Munday received his PhD in physics from Harvard University in 2008 and currently he is an assistant professor in the Department of Electrical and Computer Engineering at the University of Maryland, College Park. He is a recipient of the NSF CAREER Award, ONR YIP Award, the OSA Adolph Lomb Medal, the IEEE Photonics Society Young Investigator Award, the SPIE Early Career Achievement Award, and the NASA Early Career Faculty Space Technology Research Award.